Hexapod Type Microrobot Controlled by Power Type IC of Artificial Neural Networks

Kei Iwata, Yuki Okane, Yohei Asano, Yuki Ishihara, Kazuki Sugita, Satohiro Chiba, Satoko Ono,
Minami Takato, Ken Saito, Fumio Uchikoba
Department of Precision Machinery Engineering College of Science and Technology
Nihon University
7-24-1, Narashinodai, Funabashi, Chiba 274-8501
Japan
uchikoba@eme.cst.nihon-u.ac.jp http://www.eme.cst.nihon-u.ac.jp/~uchikoba/

Abstract: - In this paper, we report the hexapod type micro robot controlled by the neural networks. MEMS (Micro Electro Mechanical System) technology that based on the semiconductor process is used for fabrication of the microrobot. The rotational actuator is composed of four artificial muscle wires that is family of SMA (shape memory alloy). The power type bare chip IC is used for neural networks control systems of the microrobot. The IC includes 4 cell body models, 12 inhibitory synaptic models and current mirror circuits. This power type IC bare chip can output the CPG (Central Pattern Generator) waveform required for walking of the microrobot. By using power type bare chip IC, fine tuning of output current is achieved and the additional amplifier circuit is eliminated. As the result, we indicate possibility of downsizing of driving circuit and the stable actuator control. The sideways, endways, and height dimensions of the microrobot are 4.0mm, 2.7mm, and 2.5mm, respectively. The walking speed is 15mm / min and the step width is 0.6mm.

Key-Words: Microrobot, Neural networks, IC bare chip, MEMS technology, Hexapod type, Artificial muscle wire

1 Introduction

As it can work in narrow space, microrobots are expected to be active in the fields of the precision machinery engineering and medical assistance [1-3]. Conventional control system that is programed by microcomputers is effective in routine tasks of machines. However, it is difficult to control by the simple software program in the unknown place such as inside of the body, because the flexible control responding to the casual event is required for the robot in those places. In contrast, living organisms such as insects can be adaptable to various situations. The living organism acquires situations using own neural networks in the brain. To apply the biological neural networks for engineering, it is studied to model as artificial neuron model by both of the software and hardware.

The software model is easy to adjust because it uses the simulation system. However it requires long processing time. On the other hand, the hardware model can realize an immediate response. Therefore, it is possible to control robot system on a real-time by hardware model. Other research shows that controlling robots by the CPG (Central Pattern Generator) model that form cyclical behaviors of living organisms such as walking [4-6].

For miniaturization of the robot, the Micro Electro Mechanical Systems (MEMS) technology that based on the semiconductor fabrication technology is widely used [7-8]. The MEMS can realize a miniature and high accurate components [9-10]. By using MEMS many kinds of micro actuators have been developed. Particularly, methods of direct drive using the property of the materials like the shape memory alloy (SMA) and piezoelectric devices are easy to downsize because the material itself has the function of the actuator [11-12]. Although many papers concerned with these actuators has been reported, most of the moving mechanisms of the microrobot are oscillation or magnetic field and the motion is crawl. The walking motion like the insect in the small size is quite difficult.

Our purpose of the microrobot is realizing the walking with control systems of pulse-type hardware neural networks (P-HNNs). P-HNNs model are analog electronic circuits that mimic neural networks of living organisms. The previous

microrobot system reported by the presenting authors realized walking motion of hexapod type microrobot controlled by P-HNNs and succeeded in the development of integrated circuits (ICs) of P-HNNs [13-17]. However, the rotary actuators of microrobot were unstable for a long time operation because of heat accumulation around the actuator. Also, the peripheral driving circuit such as the current amplifier was too big compared with the microrobot.

Power type bare chip CPG ICs are newly developed. This IC eliminates external amplifier from the circuit board. Therefore, the size of the circuit board reduces to the comparable size to the robot itself. Also, this IC contributes to fine current tuning because of sufficient current supply. Therefore, we realize stable walking of the microrobot. After describing the mechanical structure, actuator, and CPG control system, this paper explains the power type CPG IC, results of the application.

2 Microrobot

The microrobot is required to move in various locations. The hexapod type walking robot that mimics such walking motion of ants is constructed. Fig.1 shows structure of the microrobot.

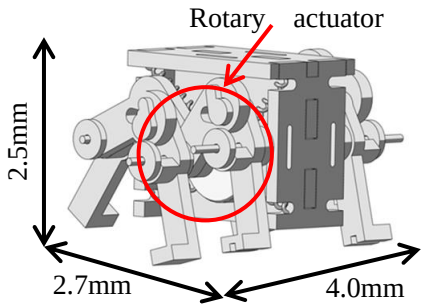

Fig.1 Design of the Micro Robot

Two rotary actuators of the mid inside of the body are connected to link mechanisms. By introducing the rotary motion of the actuator to the link mechanism, the footstep like walking motion generates. The microrobot parts are fabricated from silicon wafer by MEMS machining technology. Initially, an aluminum film of 0.1μm is formed on the silicon wafer by vacuum deposition. Pattern of the photomask expose to the resist film on the silicon wafer. Then, the resist of the unnecessary parts are dissolved and an aluminum pattern is formed by wet etching. The dry etching of the silicon wafer with the Bosch process that can etch with a high aspect ratio is used [18]. Small parts with a high accuracy can be fabricated by using this MEMS machining technology.

2.1 Actuator

Fig.2 shows the structure of rotary actuator. Four artificial muscle wires are connected to the rotor. The artificial muscle wires are composed of SMA, and shrink by joule heat of electric current. Table1 shows specification of the SMA [19]. The SMA is a spiral form and shrinkage is 50% of the original length.

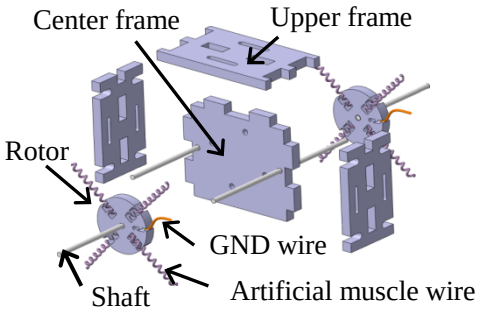

Fig.2 Structure of rotary actuator

Table 1 Specification of SMA

Coil diameter[mm]	0.2
Wire diameter[mm]	0.05
Drive current[mA]	50-120
Resistance[Ωm^{-1}]	3600
Force[gf]	3-5
Displacement[%]	50

One side of the artificial muscle wire is fixed to frame parts by bonding with cyanoacrylates adhesion. The other side is connected to the rotor part as shown in Fig.3, by conductive pastes.

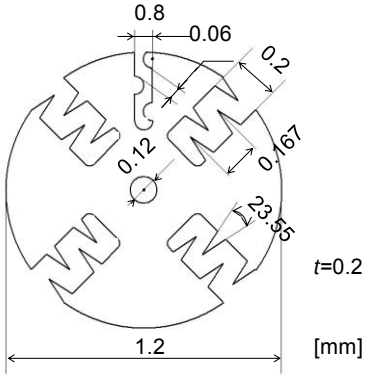

Fig.3 Dimensions of rotor part

Zigzag slits for fitting the artificial muscle wire and GND wire are formed in the rotor plates. Tungsten carbide shaft of φ0.1mm passes into a center hole of the rotor part.

A rotary motion like Fig.4 is generated by passing an electric current through an artificial muscle wire in rotation. Fig.5 shows a pulse waveform to drive the artificial muscle wire.

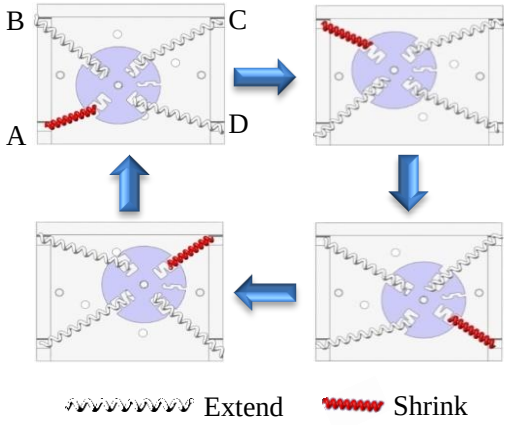

Fig.4 Rotary motion of the rotor

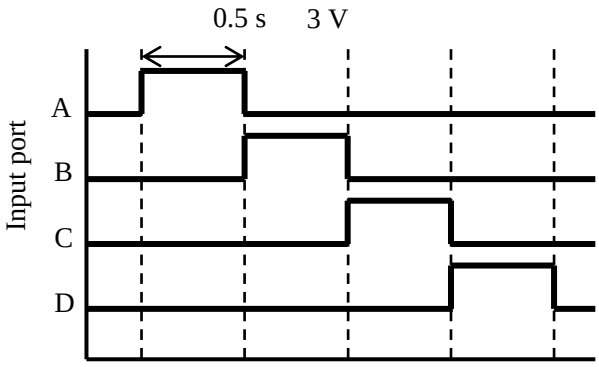

Fig.5 Driving waveform of current

2.1 Walking mechanism

Rotational motion of the actuator is transmitted to the link mechanism as shown in Fig.6. The central axis of the link mechanism is connected to the rotor, and the left and the right of the axis is fixed to the frame. The walking motion shown in Fig.7 is realized by rotation of the central shaft.

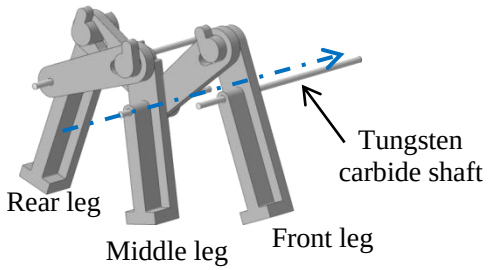

Fig.6 Link mechanism of microrobot

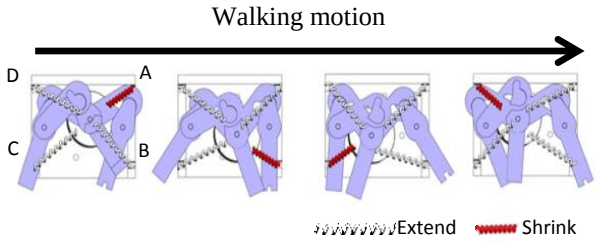

Fig.7 Walking motion of the microrobot

3 Control system

Brain of living organisms is networks of neurons. Neurons are divided into 3 areas, the cell body, the dendrite and the axon. The cell body changes the membrane potential by external stimulations and fires electrical pulses. The fired signal is transmitted to the dendrite of another neuron through the axon. The connection part of dendrites and axons is called a synapse. We use the neural networks that model the cell body and the synapse by analog circuits to the control system of the microrobot.

3.1 Neural network

Fig.8 shows circuit diagram of the cell body model. The constants of the circuit are C_G= 10μF and C_M= 2.2 μF. The cell body model that has refractory period, an analogue characteristic of the output pulse and time varying load resistance is oscillated by changing the V_A.

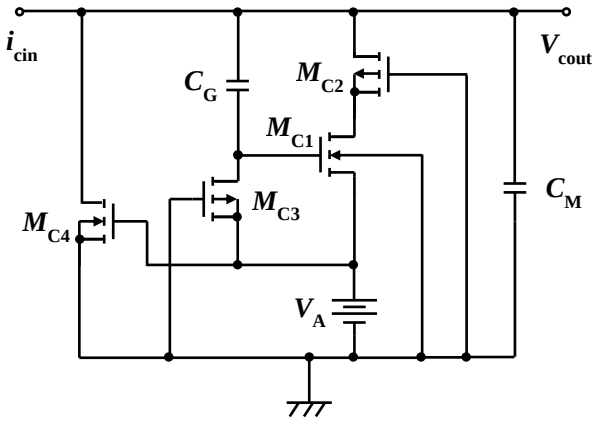

Fig.8 Circuit diagram of the cell body model.

Fig.9 shows circuit diagram of the inhibitory synapse model. Synapse model that has a spatiotemporally summation characteristics as well as living organisms adds the pulse waveform outputted by other bonded cell body model.

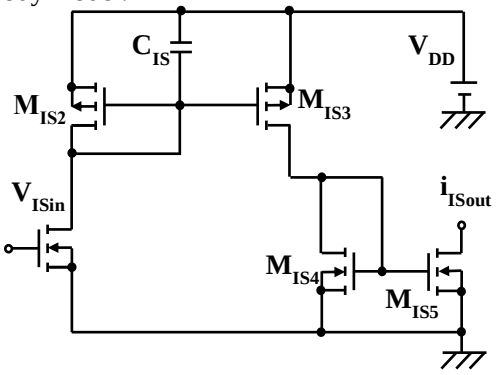

Fig.9 Circuit diagram of the inhibitory synapse model

The control system of the microrobot used in this study includes 4 cell body models (large circles), and 12 synaptic models (small closed circles) and these are coupled as shown in Fig.10. By the inhibitory synaptic model, it is possible to output the CPG waveforms of anti-phase synchronization that is necessary for walking of the micro robot.

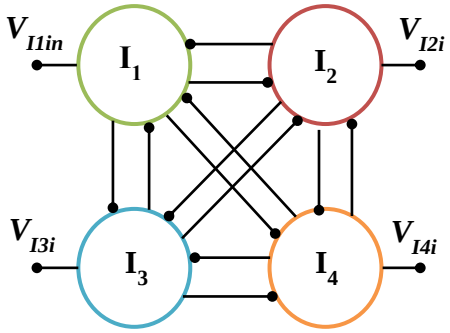

Fig.10 Circuit diagram of the inhibitory synapse model

3.2 Power type IC

The SMA shrinks by passing the current. Therefore, current mirror circuits are applied in power type IC in order to obtain a sufficient output current for walking of the microrobot. The current mirror circuit is shown in Fig.11.

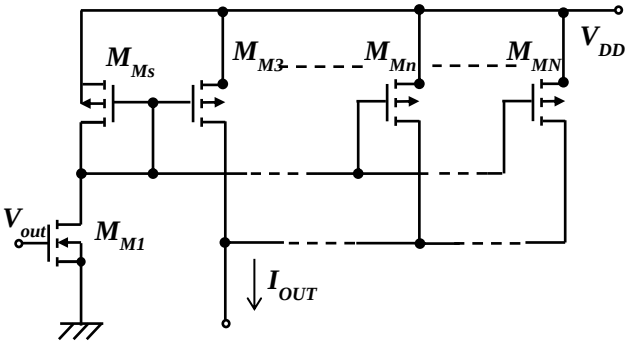

Fig.11 Circuit diagram of current mirror

Fig.12 shows pattern of power type IC. Bare chip of the power type IC is enables high current output by parallel connection of the output.

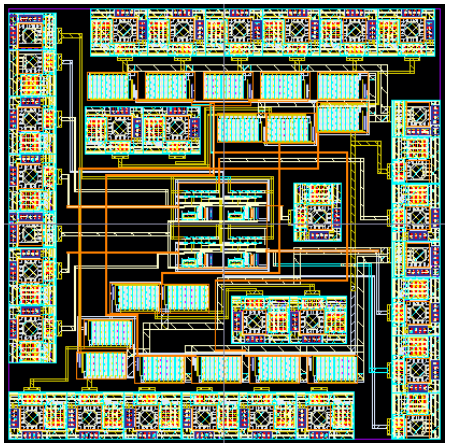

Fig.12 Pattern of power type IC

3.3 IC bare chip measurement system

Fig.13 shows the circuit diagram of the IC evaluations. Wire bonding technologies was adopted to connect the peripheral circuit and the IC bare chip.

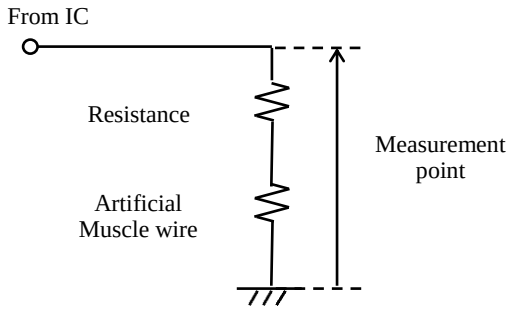

Fig.13 Evaluation circuit diagram of the power type IC

The load resistance dependence of the output current measured in the test circuit is shown in Fig. 13. Because of the transformation the output waveform by connected load resistance, V_A and V_{DD} was adjusted to obtain stable waveform.

3.4 Peripheral circuit

Fig.14 shows the amplifier used in the previous driving circuit of the microrobot. Transistors and the operational amplifiers are used for the output current amplifier and impedance matching. Four amplifiers were actually mounted on the control circuit board.

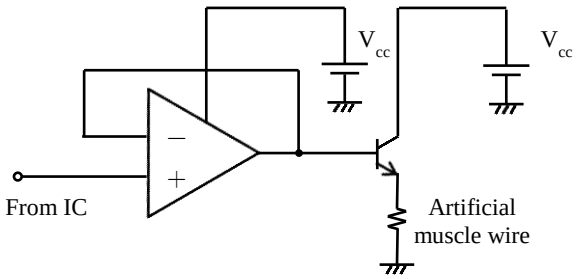

Fig.14 Previous amplifier circuit connected to IC

The power type IC include current mirror circuit used instead of the operational amplifier and the transistor. That leads to downsize the control circuit board.

4 Result and discussion

Fig.15 shows fabricated microrobot. The sideways, endways, and height dimensions of the microrobot are 4.0mm, 2.7mm, and 2.5mm, respectably.

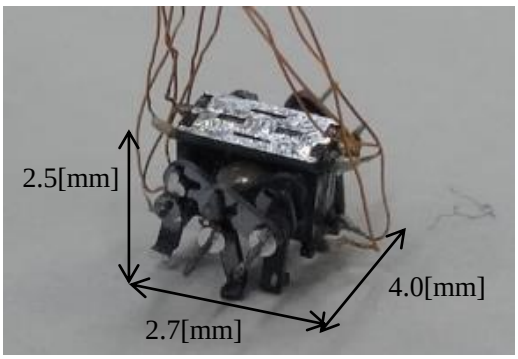

Fig.15 Fabricated the microrobot

Fig.16 shows a photograph of the fabricated parts by using the MEMS technology. The dimensional error of those parts was measured by an optical confocal microscope, and was found be always within ±3μm.

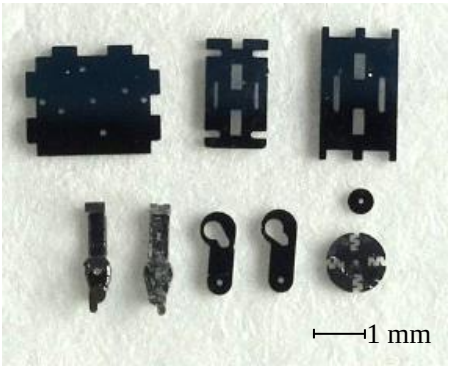

Fig.16 Fabricated parts of the microrobot

Fig.17 shows moving positions of the center axis of actuator. Applied voltage and pulse width of the waveform was 3V and 0.5s respectably. The current flowing to the SMA was 85mA by connecting a resistance for current limit. It is possible to make the rotational motion of actuator, when input current is around 85mA. Moreover, the problems that rotary motion of the actuator becomes unstable in association with the time were improved. The reason of the improvement is the suppression of the heat-up by optimising the current flow.

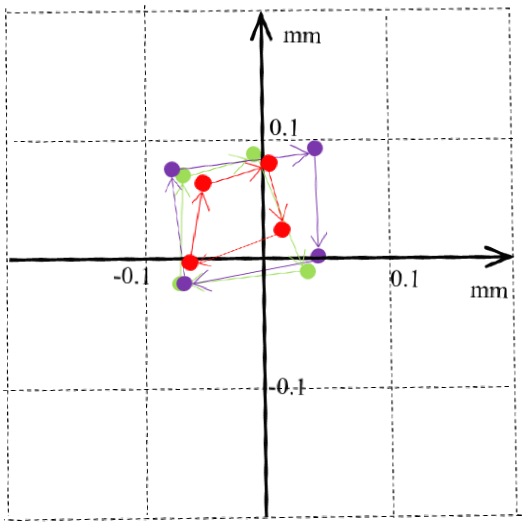

Fig.17 Positions of the center axis of actuator

Fig.18 shows the result of output current simulation of the power type IC. Input voltage of cell body model and inhibitory synapse model is 2.2V and 3V, respectably. The maximum output current was 91.2mA when the output resistance was 10Ω. It is sufficient current to drive the actuator.

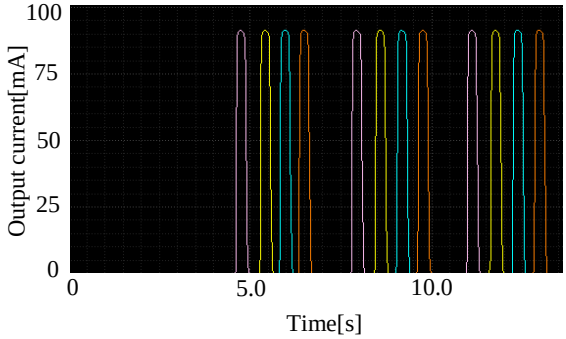

Fig.18 Result of simulation of the power type IC

Fig.19 shows the photograph of packaging IC and bare chip IC that we developed. Sizes of packaging IC and bare chip IC was 12mm square and 2.45mm square, respectively. The area was decrease by 95 percent.

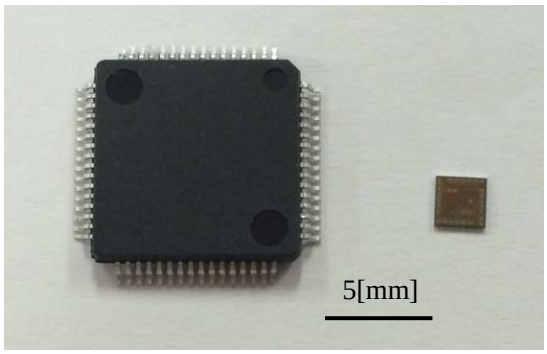

Fig.19 Photograph of the fabricated power type IC

Fig.19 shows the relationship between the load resistance and the output current. The maximum output current was 76.8mA, when load resistance value was 50Ω.

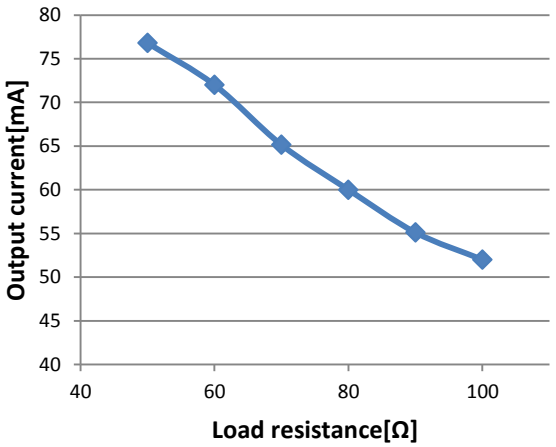

Fig.20 Relationship between the load resistance and the output current

In the robot system, the control circuit was connected to the SMA and the resistance. The total load resistance was adjusted to 50Ω. Fig. 20 shows the output waveform of the power type IC connected to the microrobot. The output waveform of reverse phase synchronization was obtained.

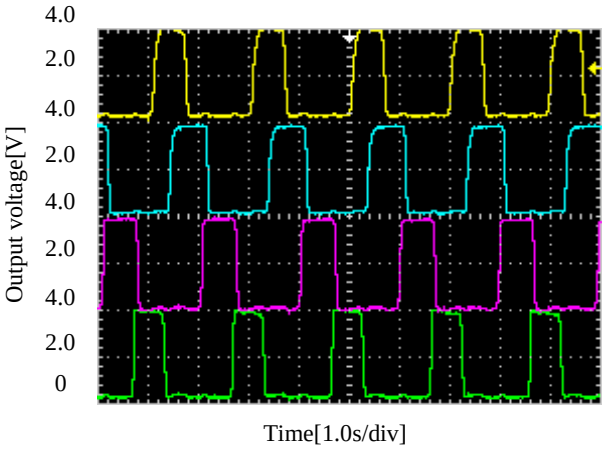

Fig.21 Output waveform of power type IC

Fig.21 shows walking motion of the microrobot controlled by the power type IC. Walking speed was 15mm / min and the step width was 0.6mm.

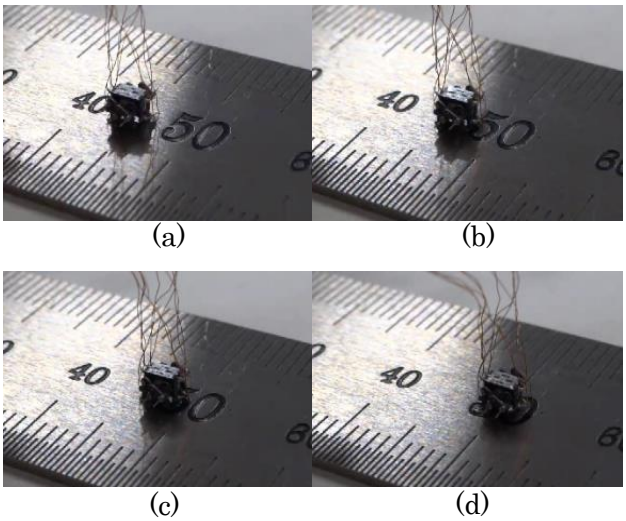

Fig.22 Walking motion of the microrobot controlled by the power type IC

5 Conclusion

In this paper, we reported the hexapod type microrobot controlled by the neural networks. The artificial muscle wire was used for the actuator of the microrobot. It became possible to drive the actuator of the microrobot for a long time by adjusting the amount of current applied to the artificial muscle wire. The sideways, endways, and height dimensions of the microrobot were 4.0mm, 2.7mm, and 2.5mm, respectably.

Power type IC bare chip containing the neural networks could output the CPG waveform required for walking of the microrobot. By using power type IC bare chip, we indicated possibility of downsizing peripheral circuit.

The footstep walking of the microrobot was succeeded by the power type IC control. The walking speed was 15mm / min and the step width was 0.6mm.

Acknowledgment:

The fabrication of the MEMS microrobot was supported by the Research Center for Micro Functional Devices, Nihon University. This study was supported by Nihon University College of Science and Technology Project Research and JSPS KAKENHI (25420226). We appreciate the support. The VLSI chip in this study has been fabricated by Digian Technology, Inc. This work is supported by VLSI Design and Education Center (VDEC), the University of Tokyo in collaboration with Synopsys, Inc., Cadence Design Systems, Inc. and Mentor Graphics, Inc.

References:

[1] T. Shibata, Y. Aoki, M. Otsuka, T. Idogaki, T. Hattori, Microwave Energy Transmission System for Microrobot, *IEICE Trans. Electron.*, 1997 Vol.E80-C, No.2, 1997, pp. 303-308.

[2] M. Takeda, Applications of MEMS Industrial Inspection, *IEEE MEMS 2001*, 2001, pp. 182-191.

[3] A. T. Baisch, P. S. Sreetharan, R. J. Wood, Biologically-inspired locomotion of a 2g hexapod robot, *Proc. of EEE IROS 2010*, 2010, pp. 5360-5365.

[4] K. Matsuoka, Mechanism of Frequency and Pattern Control in the Neural Rhythm Generators, *Biological Cybernetics*, Vol.56, 1987, pp. 345-353.

[5] T. Ikemoto, H. Nagashino, Y. Kinouchi, T. Yoshinaga, Transitions in a Four Coupled Neural Oscillator Model, *International Symposium on Nonlinear Theory and its Applications*, 1997, pp. 561-564.

[6] K. Nakada, T. Asai, Y. Amemiya, An Analog CMOS Central Pattern Generator for Interlimb Coordination in Quadruped Locomotion. *IEEE Transaction on Neural Networks*, Vol.14, 2003, pp. 1356-1365.

[7] B. R. Donald, C. G. Levey, C. D. McGray, I. Paprotny, D. Rus, An Untethered, Electrostatic, Globally Controllable MEMS Micro-Robot, *Journal of Microelectromechanical Systems*, Vol.15, 2006, pp. 1-15.

[8] E. Edqvist, N. Snis, R. C. Mohr, O. Scholz, P. Corradi, J. Gao, S. Johansson, Evaluation of Building Technology for Mass Producible Millimeter-Sized Robots Using Flexible Printed Circuit Boards, *Journal of Micromechanics and Microengineering*, Vol.19, No.7, 2009, pp. 1-11.

[9] W. C. Tang, T. H. Nguyen, R. T. Howe, Laterally Driven Poly Silicon Resonant Microstructure, *Proc. of IEEE Micro Electro Mechanical Systems. An Investigation of Micro Structures, Sensors, Actuators, Machines and Robots*, 1989, pp. 53-59.

[10] J. J. Sniegowski, E. J. Garcia, Surface-Micromachined Gear Trains Driven by an On-Chip Electrostatic Microengine, *IEEE Electron Device Letters*, Vol.17, No. 7, 1996, pp. 366-368.

[11] Y. Suzuki, K. Tani, T. Sakuhara, Development of a New Type Piezo Electric Micromotor, *Proc. of Transduceres '99*, 1999, pp. 1748-1751.

[12] P. Surbled, C. Clerc, B. L. Pioufle, M. Ataka, H. Fujita, Effect of the Composition and Thermal Annealing on the Transformation Temperature Sputtered TiNi Shape Memory Alloy Thin Films, *Thin Solid Films*, Vol.401, 2001, pp. 52-59.

[13] H. Suematsu, K. Kobayashi, R. Ishii, A. Matsuda, Y. Sekine, F. Uchikoba, MEMS Type Micro Robot with Artificial Intelligence System. *Proc. of International Conference on Electronics Packaging*, 2009, pp. 975-978.

[14] K. Okazaki, T. Ogiwara, D. Yang, K. Sakata, K. Saito, Y. Sekine, F. Uchikoba, Development of

Pulse Control Type MEMS Micro Robot with Hardware Neural Network, *Artificial Life and Robotics*, Vol.16, 2011, pp. 229-233.

[15] K. Saito, A. Matsuda, K. Saeki, F. Uchikoba, Y. Sekine, Synchronization of Coupled Pulse-Type Hardware Neuron Models for CPG Model, *The relevance of the time domain to neural network models, Springer Series on Cognitive and Neural Systems*, Vol.3, 2011, pp. 117-133.

[16] K. Saito, M. Takato, Y. Sekine, F. Uchikoba, Biomimetics Micro Robot with Active Hardware Neural Networks Locomotion Control and Insect-Like Switching Behaviour, *International Journal of Advanced Robotic Systems*, Vol.9, 2012, pp.1-6.

[17] K. Saito, M. Takato, Y. Sekine, F. Uchikoba, MEMS Microrobot System with Locomotion Rhythm Generator Using Artificial Neural Networks, *Proc. of the 1st International Conference on Robotics and Mechatronics, Structural Analysis (ROMESA 2014)*, 2014, pp. 27-32.

[18] J. K. Bhardwaj, H. Ashraf, Advanced Silicon Etching Using High-Density Plasmas, P*roc.of SPIE Micromachining and Micro fabrication Process Technology*, Vol.2639, 1995, pp. 224-233.

[19] D. Homma, Metal Artificial Muscle 'BioMetal Fiber', *Journal of the Robotics Society of Japan*, Vol.21, No.1, 2003, pp. 22-24.